

Laboratory of Computational Physics

BY LUCA CASSIA

Dipartimento di Fisica, Università di Milano-Bicocca
I-20126 Milano, Italy

Email: 1.cassia@campus.unimib.it

Table of contents

1 Hard-Core Molecular Dynamics in 2d	1
1.1 Thermalization	1
1.2 Momentum Distribution	4
1.3 Phase Transition	6
1.4 Collision Times	8
1.5 Mean Squared Displacement	9

1 Hard-Core Molecular Dynamics in 2d

In this section we simulate the dynamics of a system of N identical spherical particles in two dimensions, subject to the hard-core central potential:

$$V(r) = \begin{cases} 0 & r > R \\ \infty & r \leq R \end{cases} \quad (1)$$

with $\sigma = 2R$ being the diameter of the particles. For convenience we decide to work with adimensional quantities and rescale all lengths by the size L of the box. In these units the volume of the box itself is rescaled to 1. For the same reason we take the mass of the particles to be the reference unit of mass. Periodic boundary conditions in both directions are implemented in order to reduce boundary effects due to the finite size of the system. This turns our box in a toroidal surface.

1.1 Thermalization

First we initialize the system positioning the particles (disks) on the sites of a regular square lattice as in (Fig.1). This type of circle packing has a *packing density* η (i.e., the proportion of the surface covered by the circles) of:

$$\eta = \frac{N\pi\sigma^2}{4L^2} \quad (2)$$

which takes its maximum value for $\sigma = L/\sqrt{N}$:

$$\eta_{\max} = \frac{\pi}{4} \approx 0.78539816339... \quad (3)$$

The highest-density lattice arrangement of circles in the plane is actually the hexagonal packing

arrangement, with a maximal packing density of $\eta_h = \frac{\pi}{2\sqrt{3}} \approx 0.9069$. In fact we see that, a system with large η , spontaneously tends to arrange itself in such a way (Fig.1).

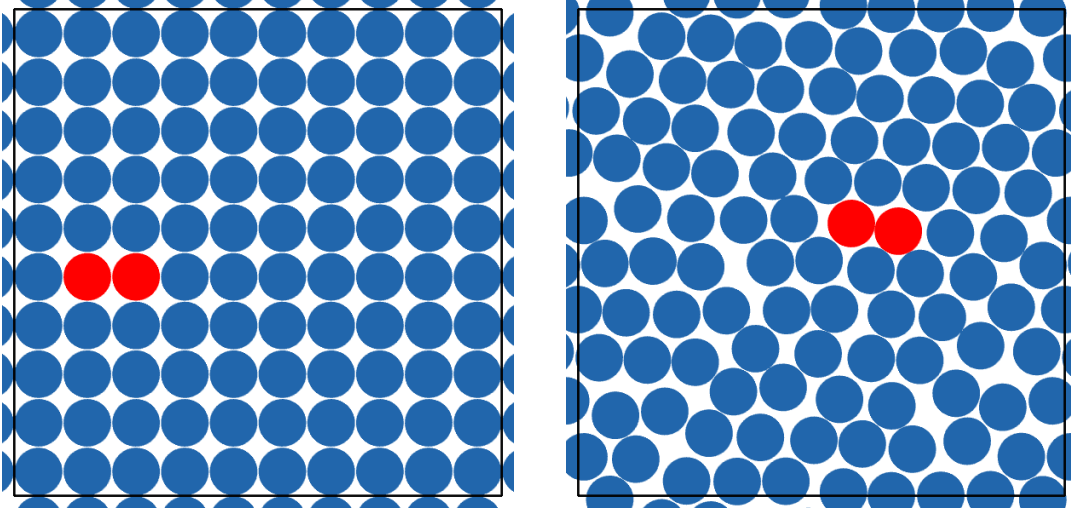


Figure 1. On the left we illustrate the initial spatial configuration of a system of 100 particles at temperature $T = 1$ and $\eta = 0.75$. On the right we show the same system after $2 \cdot 10^5$ collisions. The red disks indicate two particles colliding.

The momenta of the particles are initialized with uniform distribution inside the range $[-1, 1]$ with total momentum equal to zero (center of mass reference frame). After the initialization the momenta are rescaled in order to obtain the desired temperature. Kinetic energy and temperature are related by:

$$K = \frac{d}{2} N k_b T, \quad K = \frac{1}{2} m \sum_{i=1}^N |\vec{v}_i|^2 \quad (4)$$

$$\Rightarrow k_b T = \frac{m}{d N} \sum_{i=1}^N |\vec{v}_i|^2 \quad (5)$$

We now study the mixing properties of this type of system. We evolve a system of $N = 100$ particles from its initial configuration, for 10^4 collisions and measure the pressure (Fig.2) and the mean free path (Fig.3) every 10 collisions. This procedure is also repeated for $N = 400$.

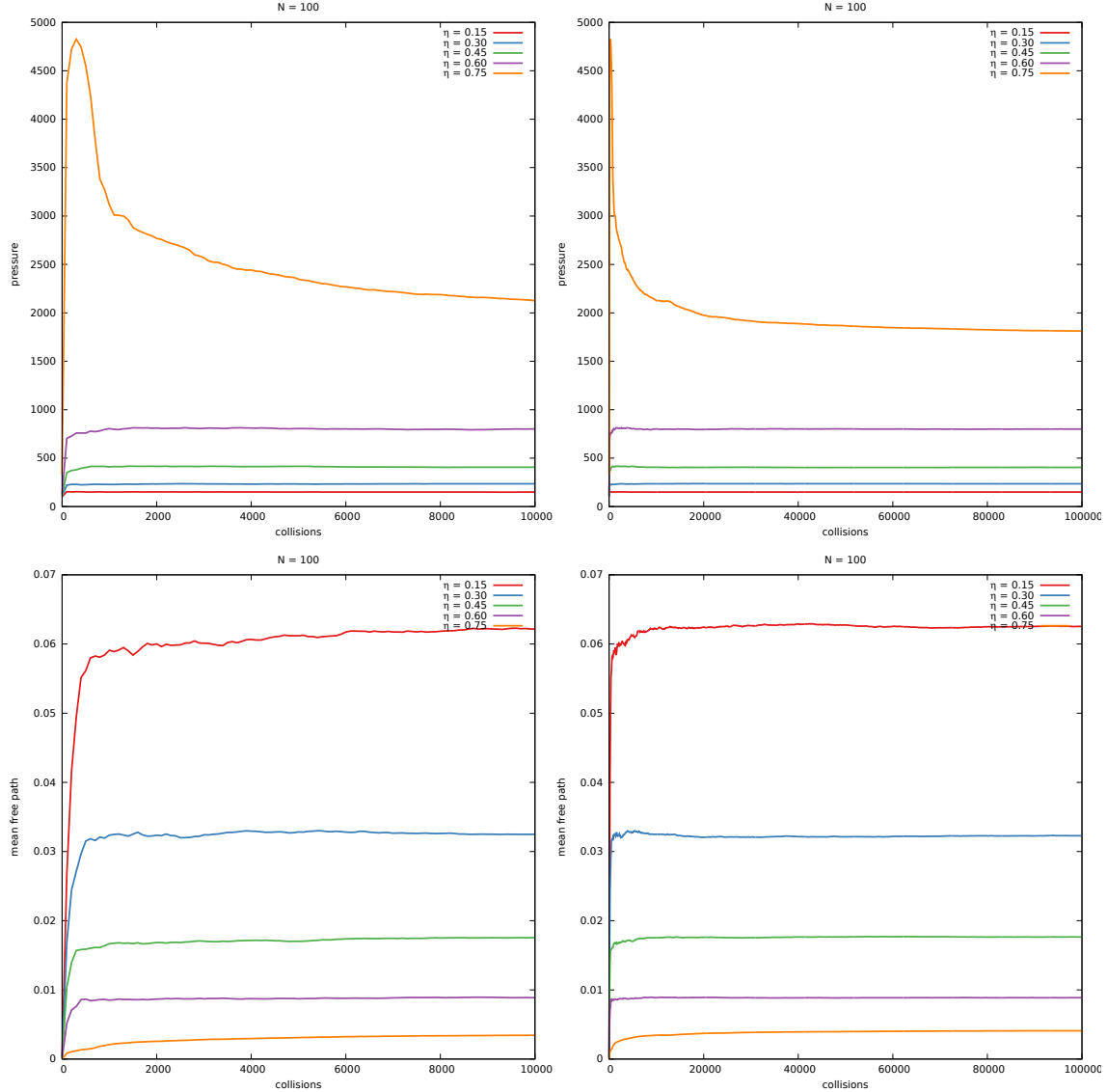


Figure 2. Plot of the thermalization process of an hard-core interacting gas of $N = 100$ particles. The top two figures illustrate the pressure as a function of the number of collisions, while the bottom two show the mean free path of the particles. Different colors represent the different values of $\eta = 0.15, 0.30, 0.45, 0.60, 0.75$ used for the simulations. On the right is the same process, after a larger number of collisions. The mixing rate of the system (as a function of the number of collisions) grows with η and the number of particles.

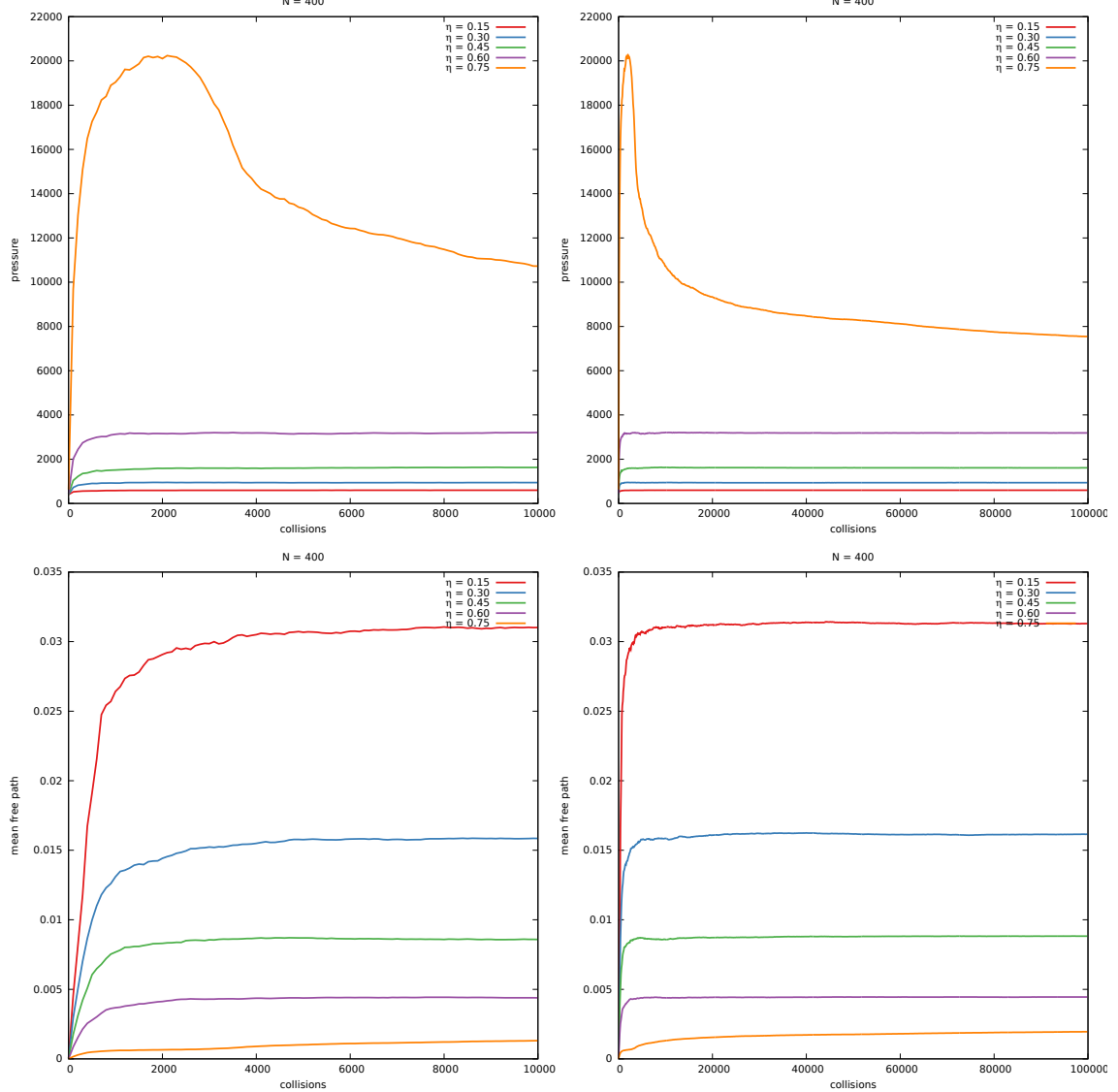


Figure 3. Plot of the thermalization process of an hard-core interacting gas of $N = 400$ particles. The mixing of this larger system is much slower.

A many-body system reaches thermalization only when every particle has interacted with every other particle at least once. Since hard-core particles interact only when they collide with each other, the mixing of this type of systems depends only on the number of collisions and not directly on the elapsed time.

We see that larger systems (system with a large number of particles) need more collisions to mix completely, especially at high densities η , while smaller systems mix faster. At high densities we also note a peak in the pressure curve near the start of the simulation. This is due to the fact that we used an initial arrangement not ideal for the close packing of particles. The particles are initially very close to each other and interact frequently, but after a few collisions they rearrange in such a way as to maximize the distance between them, therefore reducing the pressure (Fig.1).

If we work with $N = 100$ particles, we can consider the system thermalized after $5 \cdot 10^5$ collisions.

1.2 Momentum Distribution

After thermalization is reached, the system acquires time translation invariance and the distribu-

tion of the momenta of the particles converge to the Maxwell-Boltzmann distribution:

$$f(v) = \sqrt{\left(\frac{m}{2\pi k_b T}\right)^3} 4\pi v^2 \exp\left[-\frac{mv^2}{2k_b T}\right] \quad (6)$$

and for the single components:

$$f(v_i) = \sqrt{\frac{m}{2\pi k_b T}} \exp\left[-\frac{mv_i^2}{2k_b T}\right] \quad (7)$$

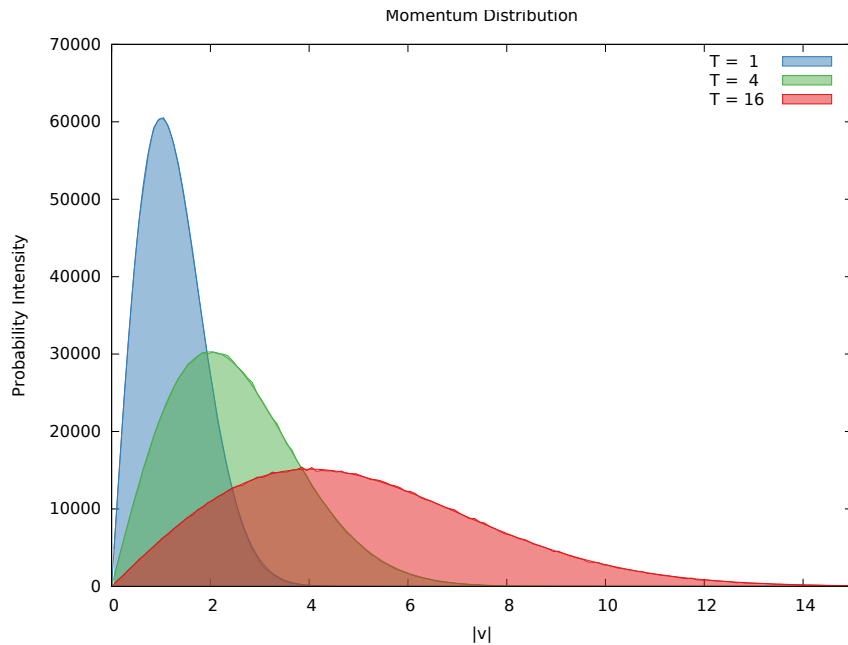


Figure 4. Histogram of the modulus of the momenta for $N = 100$ particles at $\eta = 0.5$. The measurements are taken after $5 \cdot 10^4$ collisions from the start of the simulation, and after that every 500 collisions for a total of 10^4 datasets each containing the momenta of N particles. The system is initialized at temperatures $T = 1, 4, 16$.

We repeat the simulation for three different values of the temperature ($T = 1, 4, 16$) which we set by hand at the beginning. The temperature can then be read from a fit of the histograms of (Fig.4) and compared with the one obtained from (5):

T	T_{fit}
1	1.011343 ± 0.005696
4	4.028977 ± 0.007747
16	16.134445 ± 0.023048

We also plot the distribution for the single components v_x and v_y :

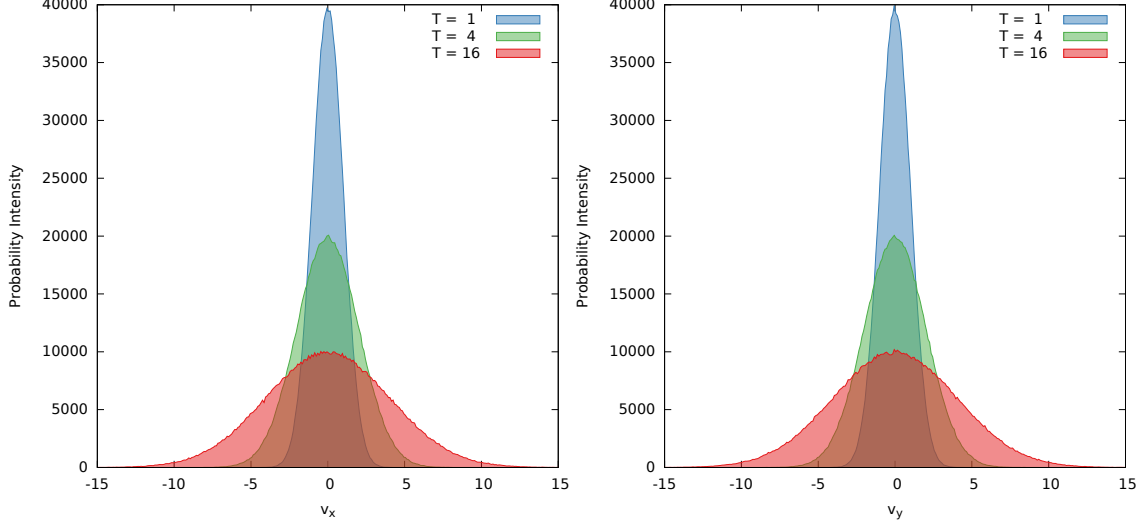


Figure 5. Histograms of the x (left) and y (right) components of the momenta for $N = 100$ particles.

Remark: in this section we decide not to use adimensional units for time t and temperature k_bT otherwise we would end up with only one distribution with $k_bT = 1$. What we do is to set only $k_b = 1$, this way we still have the freedom to set the temperature T by rescaling all the momenta (and hence rescale time t of the right amount in order to balance the change in T). For all the following sections we use the rescaling $L = 1, m = 1$ and $k_bT = 1$ such that:

$$K = \frac{d}{2} N \quad (8)$$

1.3 Phase Transition

In this section we study the η dependence of some interesting quantities describing the system. First we look at the pressure P as the packing density is increased. For a system such as those in consideration, we define the pressure P using the formula:

$$\frac{PV}{Nk_bT} = 1 + \frac{1}{2Kt} \sum_{c=1}^{N_c} m \sigma |\Delta \vec{v}_{ij}(t_c)| \quad (9)$$

with $m\Delta \vec{v}_{ij}(t_c)$ being the exchanged momentum in the collision taking place at time t_c , N_c the total number of collisions and t the runtime of the simulation.

Remark: as a measure against autocorrelation effects we decide to sample data each from an independent run and then take the average over all runs (at the same η).

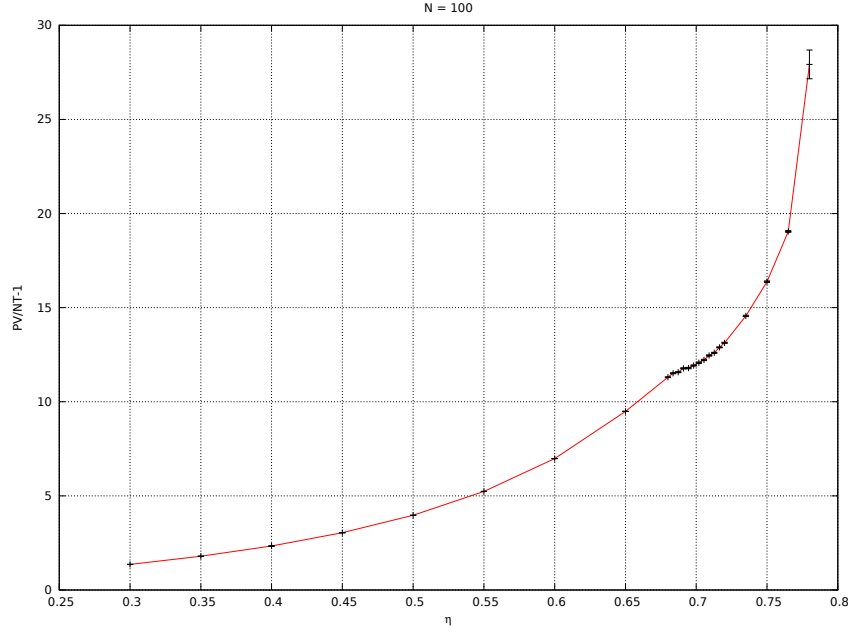


Figure 6. Plot of $\frac{PV}{Nk_bT} - 1$ as a function of η for a system of 100 particles. Every measurement is taken from the average of 50 independent runs each collected after an initial thermalization time of $5 \cdot 10^4$ collisions. The errorbars represent the standard errors of the averages. At large values of η (~ 0.75) the system takes more time to reach thermal equilibrium and this means that measurements are collected when the system is not yet completely mixed. For this reason larger fluctuations are introduced between different simulation runs and the errors are greater.

Near $\eta = 0.7$ we observe a first order phase transition characterized by a discontinuity in the pressure with respect to the thermodynamic variable η . The system is found in a liquid phase for values of the density $\eta < 0.7$ and in a solid phase for $\eta > 0.7$. This kind of phase transition displays a plateau region where the transition takes place. In fact there is no well defined critical point since multiple phases can coexist near the transition.

We also note that, since the hard-core potential has no attractive effect on the particles, there cannot be a phase transition with respect to the temperature. The order-disorder transition we observe is purely of geometrical nature.

Another thermodynamic quantity that shows discontinuity at the phase transition is the mean free path, i.e., the average distance traveled by a particle between successive impacts:

$$l_c = \sum_{c=1}^{N_c^i} \frac{|\Delta \vec{r}_i(t_c, t_{c-1})|}{N_c^i} \quad (10)$$

To compute l_c , we save the total distance travelled by every particle $\sum |\Delta \vec{r}_i| \sim \int |d\vec{r}_i|$ and the total number N_c^i of collisions it had during its path.

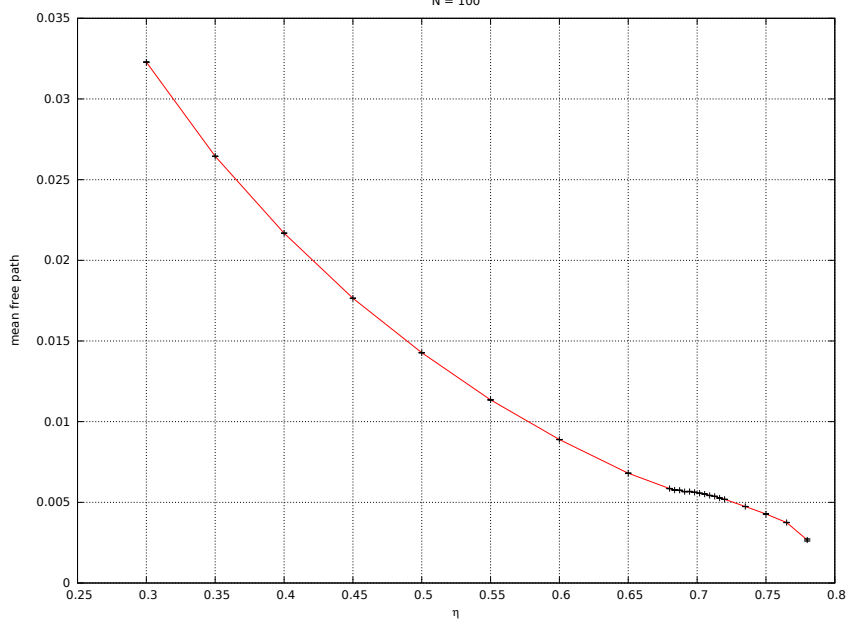


Figure 7. Plot of the mean free path against η for $N = 100$.

We also plot the distribution of the mean free path:

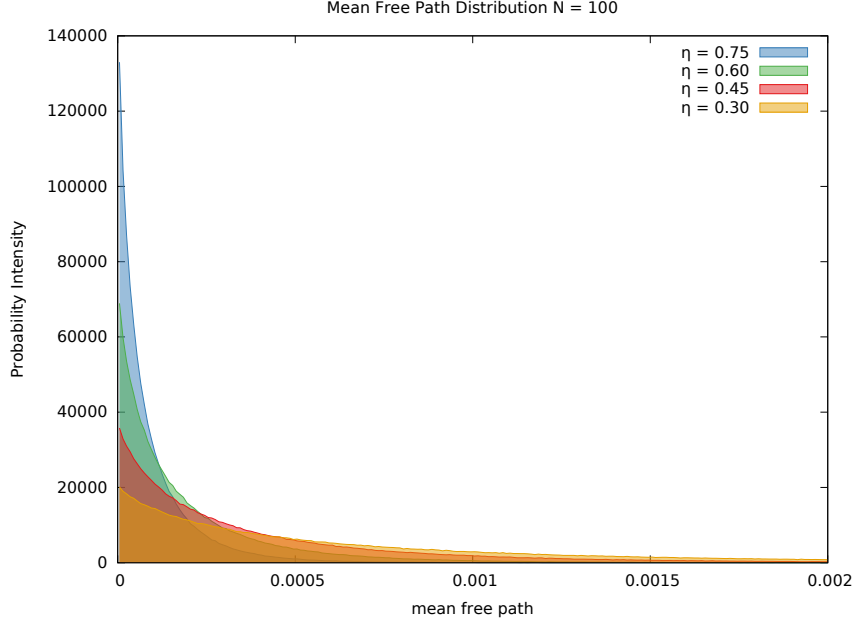


Figure 8. Distribution of the mean free path l_c for $N = 100$ and $\eta = 0.30, 0.45, 0.60, 0.75$. The histograms are obtained from a sample of 10^6 measurements and after a thermalization time of $5 \cdot 10^4$ collisions.

1.4 Collision Times

Yet another interesting quantity to look at is the collision time t_c , i.e., the time between two consecutive collisions. In (Fig.9) we present the distribution of t_c for increasing values of η :

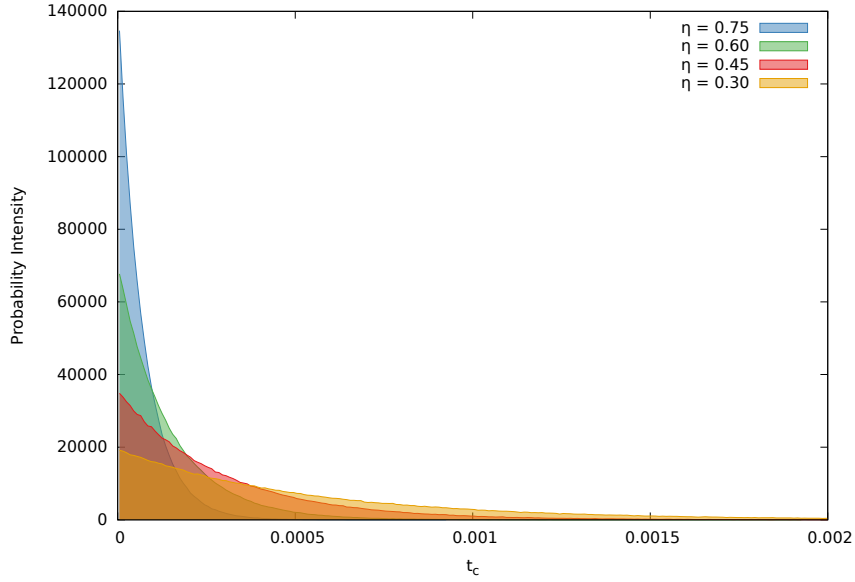


Figure 9. Distribution of the collision time t_c for $N = 100$ and $\eta = 0.30, 0.45, 0.60, 0.75$. The histograms are obtained from a sample of 10^6 measurements and after a thermalization time of $5 \cdot 10^4$ collisions.

As the density of particles increases, the collisions become more frequent because of the decrease in free space available for the particles to freely travel. This implies that the distribution of the collision times must become narrower for larger values of η (Fig.9).

Similarly to the case of the pressure and the mean free path, t_c also has a discontinuity at the phase transition, as we can see from (Fig.10):

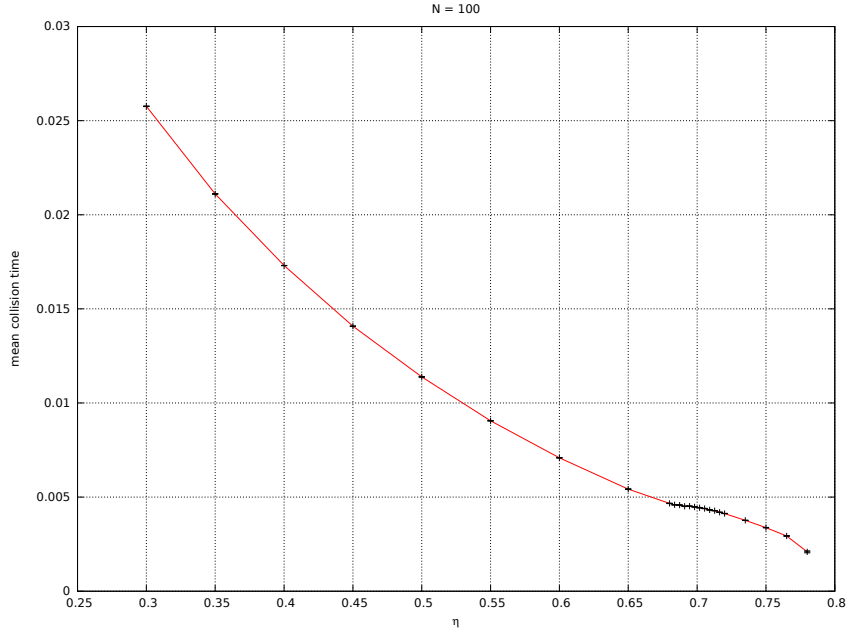


Figure 10. Plot of the mean collision time $\langle t_c \rangle$ against η for $N = 100$.

1.5 Mean Squared Displacement

The mean squared displacement (MSD), defined as:

$$\text{MSD} = \langle (\vec{r}_i(t) - \vec{r}_i(t_0))^2 \rangle = \langle \Delta \vec{r}(t, t_0)^2 \rangle \quad (11)$$

is a very common measure of the amount of the system “explored” by a particle as the time passes. For diffusion processes (random walks), the MSD grows linearly with time:

$$\text{MSD} \simeq 2 d D \Delta t \quad \text{Einstein's relation} \quad (12)$$

where d is the dimension of the space and D is the self-diffusion constant. Usually one would plot the MSD as a function of time and, in the limit of large times, a linear fit of the curve would yield the diffusion coefficient of the process. However, we will see that the use of periodic boundary conditions will affect the linearity of (12). In fact, when a particle travels around a closed loop of non trivial homology, the total displacement computed by (11) is approximately zero, while actually the particle has travelled a distance of the order of the size L of the system. This phenomenon will effectively confine the particle to a finite volume, and as a consequence, the MSD will reach a plateau value. It is this plateau value that provides the definition of D for a finite system.

For large Δt this value can be computed exactly: let $f_i(\vec{r}_0, \vec{r}, t_0, t)$ be the probability of a particle to go from \vec{r}_0 to \vec{r} after a time $\Delta t = t - t_0$, then:

$$\langle (\vec{r}_i(t) - \vec{r}_i(t_0))^2 \rangle = \int_V d\vec{r} \int_V d\vec{r}_0 (\vec{r} - \vec{r}_0)^2 f_i(\vec{r}_0, \vec{r}, t_0, t) \quad (13)$$

$$f(\vec{r}, t) = \int_V f_i(\vec{r}_0, \vec{r}, t_0, t) d\vec{r}_0, \quad f(\vec{r}, t) = \int_V f_i(\vec{r}_0, \vec{r}, t_0, t) d\vec{r}_0, \quad f(\vec{r}_0, t_0) = f(\vec{r}, t) = \frac{1}{V} \quad (14)$$

where the first two equalities are just the definitions of the marginal probability distributions and the last is a consequence of spatial and temporal homogeneity at thermal equilibrium.

After a long time has passed, the particle loses every information about its past, and the joint probability distribution factorizes:

$$f_i(\vec{r}_0, \vec{r}, t_0, t) \xrightarrow{\Delta t \rightarrow \infty} f_i(\vec{r}_0, t_0) f_i(\vec{r}, t) \quad (15)$$

The MSD can then be computed for large time separations as:

$$\begin{aligned} \langle \Delta \vec{r}(t, t_0)^2 \rangle &= \int_V d\vec{r} \int_V d\vec{r}_0 (\vec{r} - \vec{r}_0)^2 f_i(\vec{r}_0, t_0) f_i(\vec{r}, t) \\ &= \int_V d\vec{r} \int_V d\vec{r}_0 (|\vec{r}|^2 - 2\vec{r} \cdot \vec{r}_0 + |\vec{r}_0|^2) f_i(\vec{r}_0, t_0) f_i(\vec{r}, t) \\ &= \frac{1}{V} \int_V d\vec{r} |\vec{r}|^2 - 2 \langle \vec{r}(t) \rangle \cdot \langle \vec{r}_0(t_0) \rangle + \frac{1}{V} \int_V d\vec{r}_0 |\vec{r}_0|^2 \\ &= \frac{2}{V} \int_V d\vec{r} |\vec{r}|^2 \end{aligned} \quad (16)$$

Where the factor 2 in the last step, counts both the displacement of \vec{r} and \vec{r}_0 , since they are independent. We can fix the initial position of the particle to be 0 for convenience and then look only at the displacement with respect to that position. This is equivalent to considering only the final position contribution, which is half the MSD of (16).

Finally, for a volume $V = L^d$, we obtain:

$$\begin{aligned} \langle \Delta \vec{r}(t, t_0)^2 \rangle &= \frac{1}{V} \int_V d\vec{r} |\vec{r}|^2 \\ &= \frac{1}{L^d} \int_{-L/2}^{L/2} dx_d \dots \int_{-L/2}^{L/2} dx_2 \int_{-L/2}^{L/2} dx_1 (x_1^2 + x_2^2 + \dots + x_d^2) \\ &= \frac{1}{L^d} L^{d-1} \frac{2d}{3} \left(\frac{L}{2} \right)^3 = \frac{d}{12} L^2 \xrightarrow{L=1} \begin{cases} 1/6, & d=2 \\ 1/4, & d=3 \end{cases} \end{aligned} \quad (17)$$

By using the time translation invariance of the system (at thermalization) and the fact that all the particles are identical, we can compute an estimate of the MSD by averaging over every time interval $[t, t + \Delta t]$ and every particle i :

$$\text{MSD}(\Delta t) = \frac{1}{N} \sum_{i=1}^N \frac{1}{(t_S - \Delta t - t_0 + 1)} \sum_{t=t_0}^{t_S - \Delta t} [\vec{r}_i(t + \Delta t) - \vec{r}_i(t)]^2 \quad (18)$$

with t_S being the time of the simulation.

We see from (Fig.11) that initially the curves grow linearly with the time separation as one would expect for a diffusive process. For larger separations, though, the MSD reaches the plateau of (17) and fluctuate around it. The measurement taken at very large displacements ($\Delta t \approx t_S$) are of little significance because of the reduced amount of statistics we can collect:

$$N_{\text{samples}}(\Delta t) = (t_S - \Delta t - t_0 + 1) \xrightarrow[t \sim t_S]{} 1$$

We can also see the phase transition of the system in the abrupt drop in the self-diffusion coefficient of the initial diffusive parts of the curves¹.

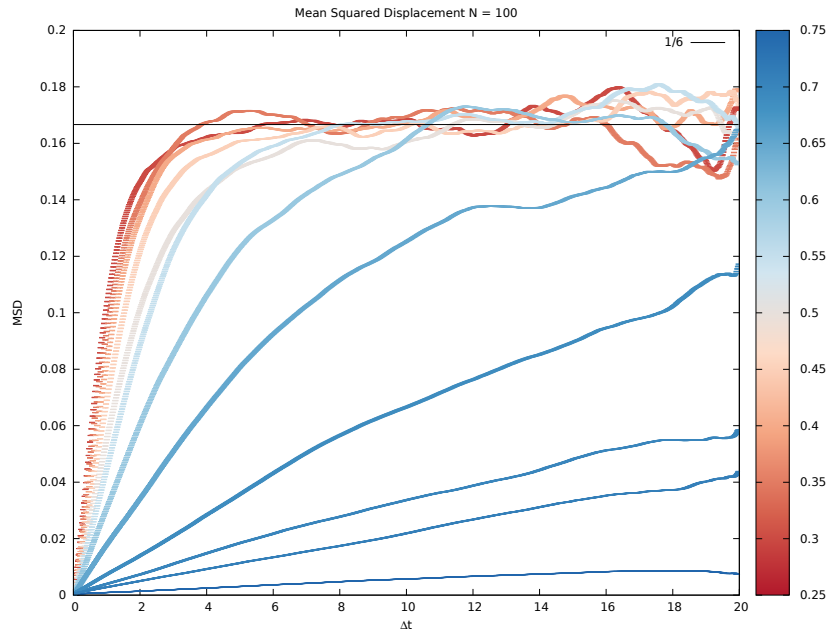


Figure 11. Mean squared displacement from a simulation of $N = 100$ particles. The measurements are taken for a simulation time $t_S = 20$ with a time step of 0.003 after a thermalization of $5 \cdot 10^4$ collisions. The color palette represents different values of η . The solid line in black is the exact result for $\Delta t \rightarrow \infty$.

As η approaches large values, the particles are more and more constrained by the increase in occupied volume and are less free to travel around (Fig.13). As a consequence they resent much later of the finite size effect of the system, and continue to diffuse linearly with time for much longer (Fig.12):

¹. As already mentioned in (12), the first derivative of the MSD with respect to time is proportional to the self-diffusion coefficient D .

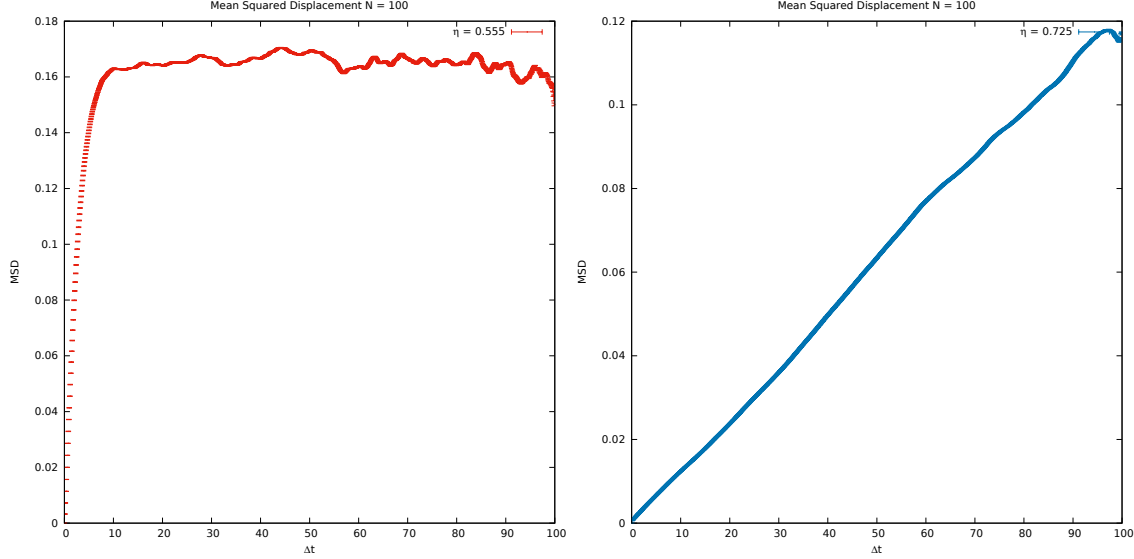


Figure 12. Mean squared displacement from a simulation of $N = 100$ particles at $\eta = 0.555$ and $\eta = 0.725$. The measurements are taken for a simulation time $t_S = 100$ with a time step of 0.01 after a thermalization of $5 \cdot 10^4$ collisions.

This is intuitively understood by looking at the trajectory on the right of (Fig.13) and realizing that the particle lives mostly in the bulk of the box and that it almost never travels around a loop of non trivial homology.

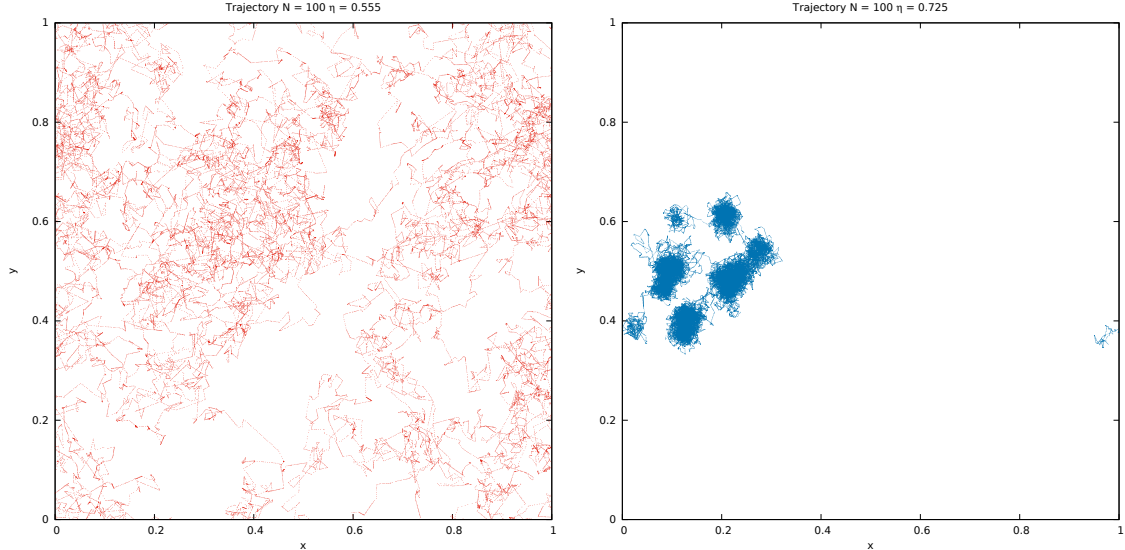


Figure 13. Trajectory of a single particle at $\eta = 0.555$ (left) and $\eta = 0.725$ (right) in a system with $N = 100$. Both simulations had a runtime of $t_S = 100$ after a thermalization time corresponding to $5 \cdot 10^4$ collisions.

Another approach is to consider the “unfolded” history (or unfolded coordinates) of the particles, i.e., the trajectories that the particles would have followed if there were no periodic boundary conditions but with the same collisions happening in the “folded” history². The effect of using unfolded coordinates is immediately visible from the plot of the MSD (Fig.15). Having removed the effect of the boudary conditions, the diffusive nature of the process is preserved even at large time intervals, especially for $\eta \ll 1$ where the confinement of the plateau $1/6$ was most evident.

². The term “folding” refers to the procedure of obtaining a torus from a quotient of the two-plane, usually the complex plane \mathbb{C} . Conversely, the unfolding corresponds to the inverse procedure of obtaining a plane from copies of a torus.

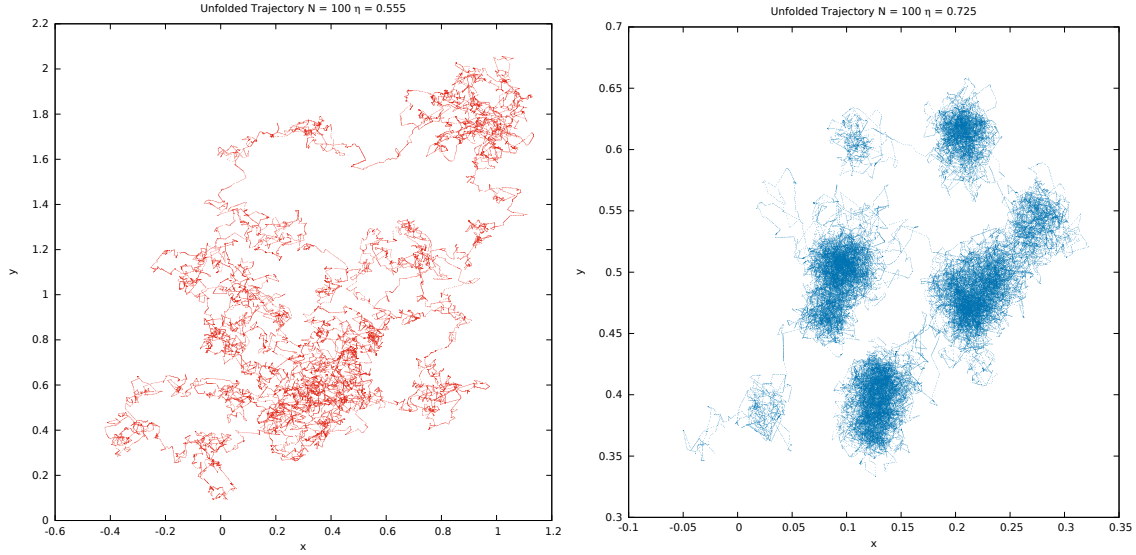


Figure 14. Trajectories of the same particles of (Fig.13) but in unfolded coordinates.

As we can see, the unfolding procedure is most effective for lower values of the density, when the particles have more freedom of movement and can cross many times the boundaries from many directions.

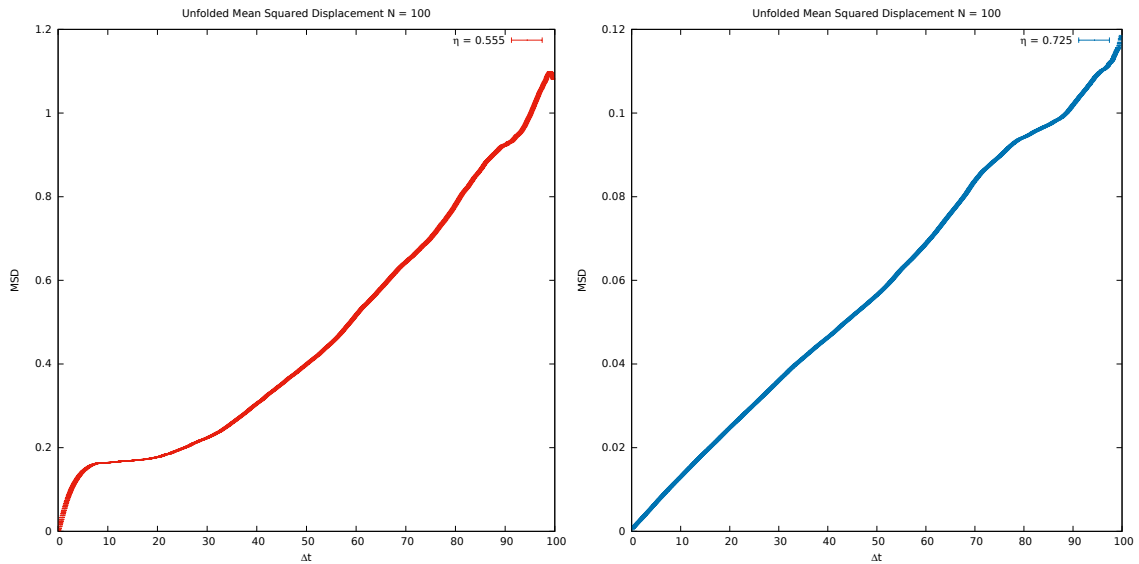


Figure 15. Mean squared displacement from an unfolded simulation of $N = 100$ particles at $\eta = 0.555$ and $\eta = 0.725$. The measurements are taken for a simulation time $t_S = 100$ with a time step of 0.01 after a thermalization of $5 \cdot 10^4$ collisions.